OMTN, Volume *27*

Supplemental information

Heterogeneity of human corneal endothelium implicates lncRNA *NEAT1* in Fuchs endothelial corneal dystrophy

Qun Wang, Shengqian Dou, Bin Zhang, Hui Jiang, Xia Qi, Haoyun Duan, Xin Wang, Chunxiao Dong, Bi Ning Zhang, Lixin Xie, Yihai Cao, Qingjun Zhou, and Weiyun Shi

Supplemental Information

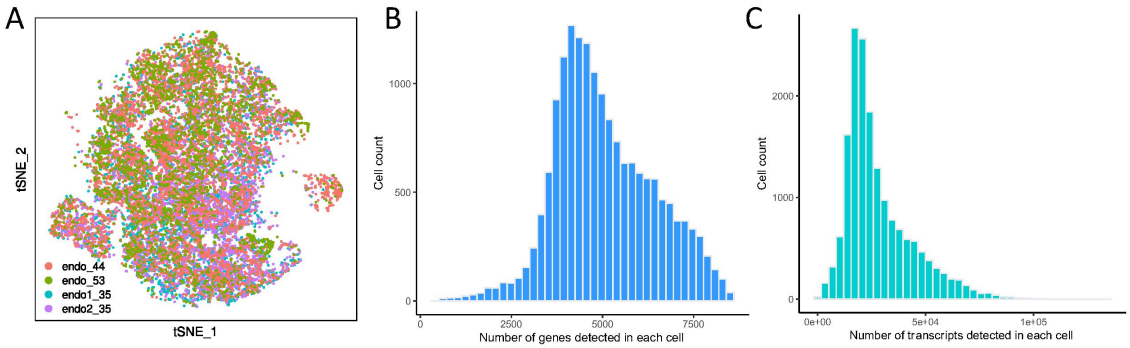

Figure S1. Sampling information and quality control for each library. A. t-SNE clustering of human corneal endothelial cells colored by sample origins. B. Distribution of the cell number versus the number of detected genes. C. Distribution of the cell number versus the number of transcripts.

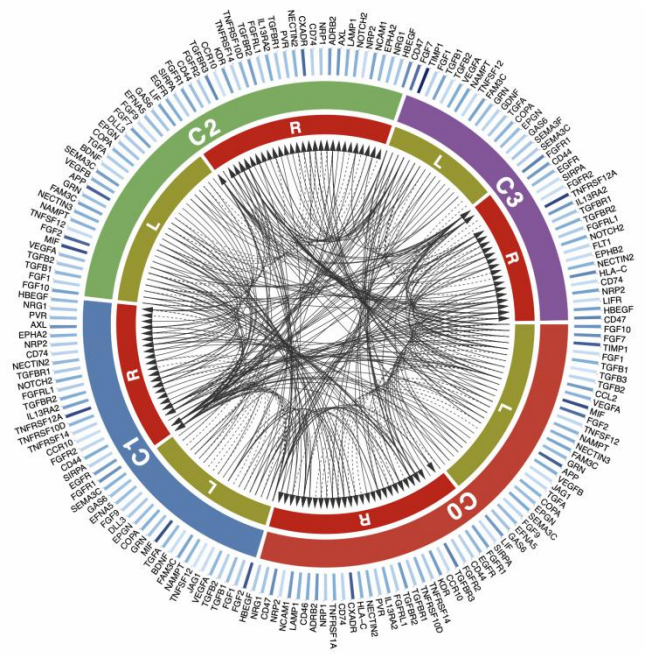

Figure S2. Circular plot displays the putative communications between corneal endothelial subtypes. Lines originate at the ligand and connect to its receptor as indicated by the arrowhead.

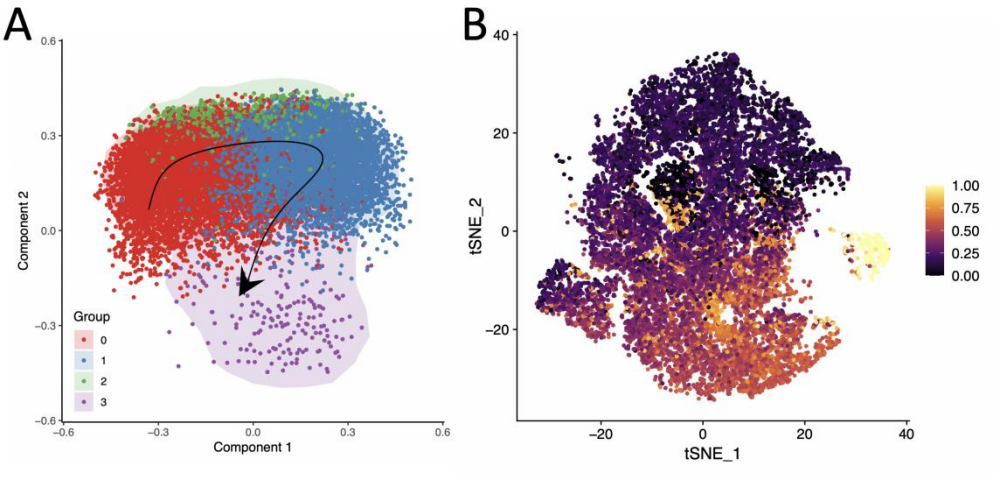

Figure S3. Pseudotemporal dynamics analysis of heterogenous corneal endothelial cells. A. Cell trajectories on pseudotime of corneal endothelial cells generated by SCORPIUS. B. Projection of pseudotime trajectories onto the t-SNE space.

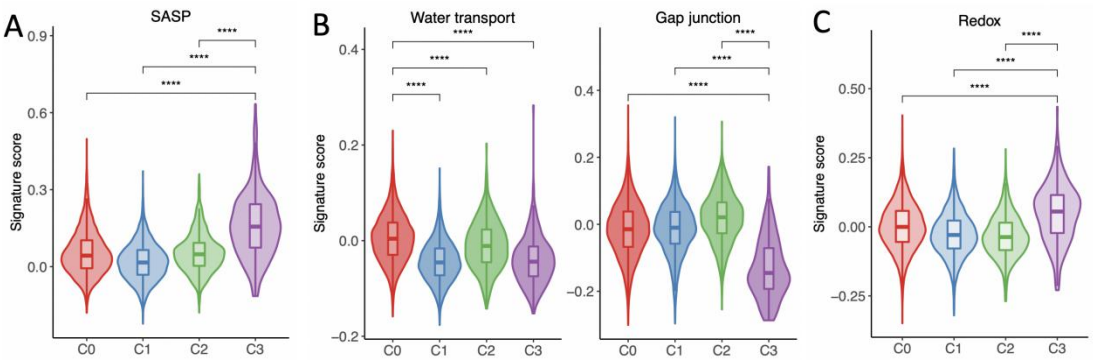

Figure S4. Transcriptional signatures of four endothelial cell subtypes. A-C. Gene scoring analysis using curated molecular signatures for SASP (A), endothelial functions (B) and Redox process (C). ****, $p < 0.0001$ (two-sided Wilcoxon rank-sum tests).

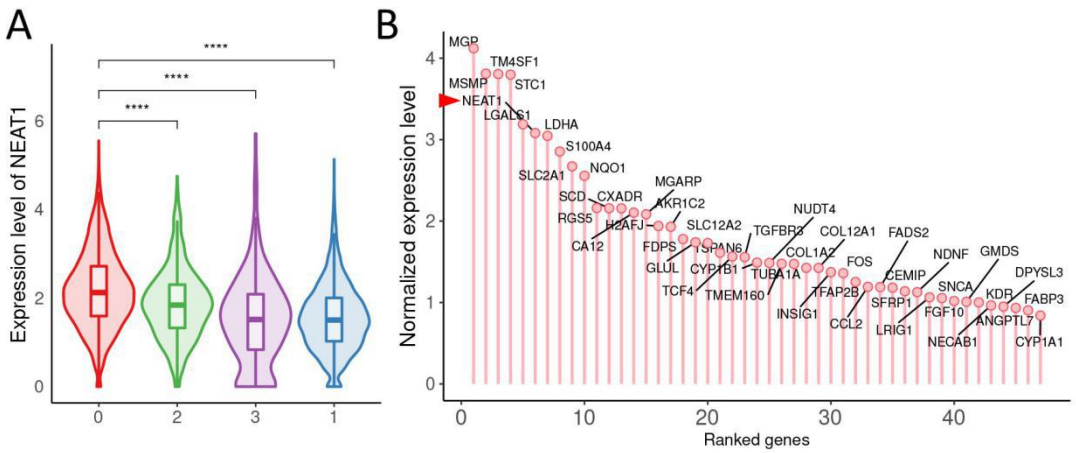

Figure S5. (A) The expression level of *NEAT1* across corneal endothelial subtypes. ****, $p < 0.0001$ (two-sided Wilcoxon rank-sum tests). (B) Normalized expression level of top 50 genes in C0 cells. All genes were ranked along x-axis by the expression level.

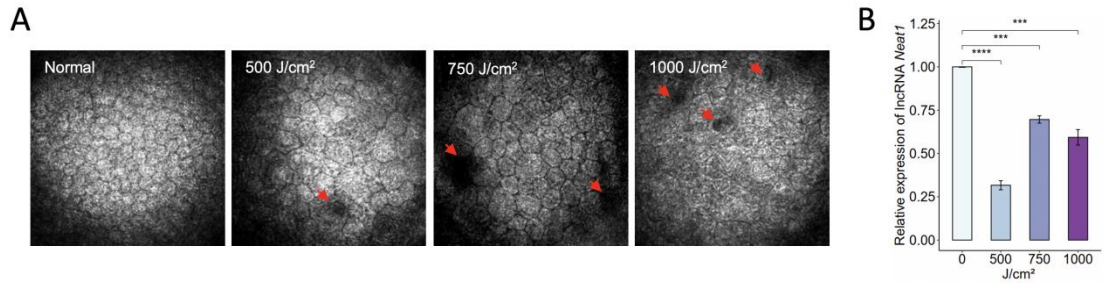

Figure S6. *Neat1* was suppressed in UVA irradiation-induced FECD mouse cornea. (A) *In vivo* confocal HRT photographs of mouse CE 1 month post-500, 750, 1000 J/cm^2 UVA. (B) The qRT-PCR was performed to evaluate *Neat1* expression using the CE tissues from the normal and FECD mouse. Quantitative data are shown as the mean±SE, n=3 for each group. ***, $p<0.001$; ****, $p<0.0001$ (two-tailed t test).

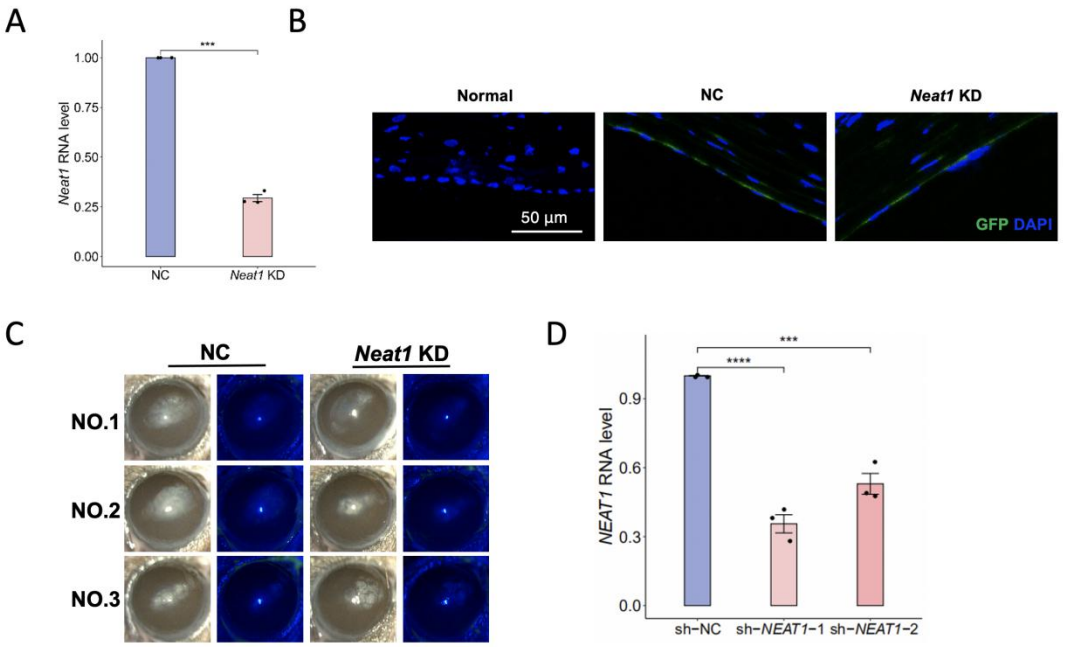

Figure S7. Intracameral injection of rAAV silencing endogenous *Neat1* in mouse CE and shRNA-mediated *NEAT1* knockdown in human corneal endothelial cells. (A) The relative expression of *Neat1* between silencing control (NC) and silencing *Neat1* group (*Neat1* KD). n=3 for each group; ***, p<0.001 (two-tailed t test). (B) GFP expression in rAAV-injected mouse CE. Scale bars, 50 μm. (C) Representative slit lamp images showing mouse corneal clarity and fluorescein staining of the corneal epithelial surface 3 months post 500 J/cm^2 UVA. (D) Verification of efficiency by qRT-PCR upon shRNA-mediated *NEAT1* knockdown in CEnCs. Data are presented as the mean±SE. n=3 for each group. ***, p < 0.001; ****, p < 0.001 (two-tailed t test). sh-NC, scrambled control shRNA; sh-*NEAT1*-1 and sh-*NEAT1*-2, two different *NEAT1* shRNA duplexes.

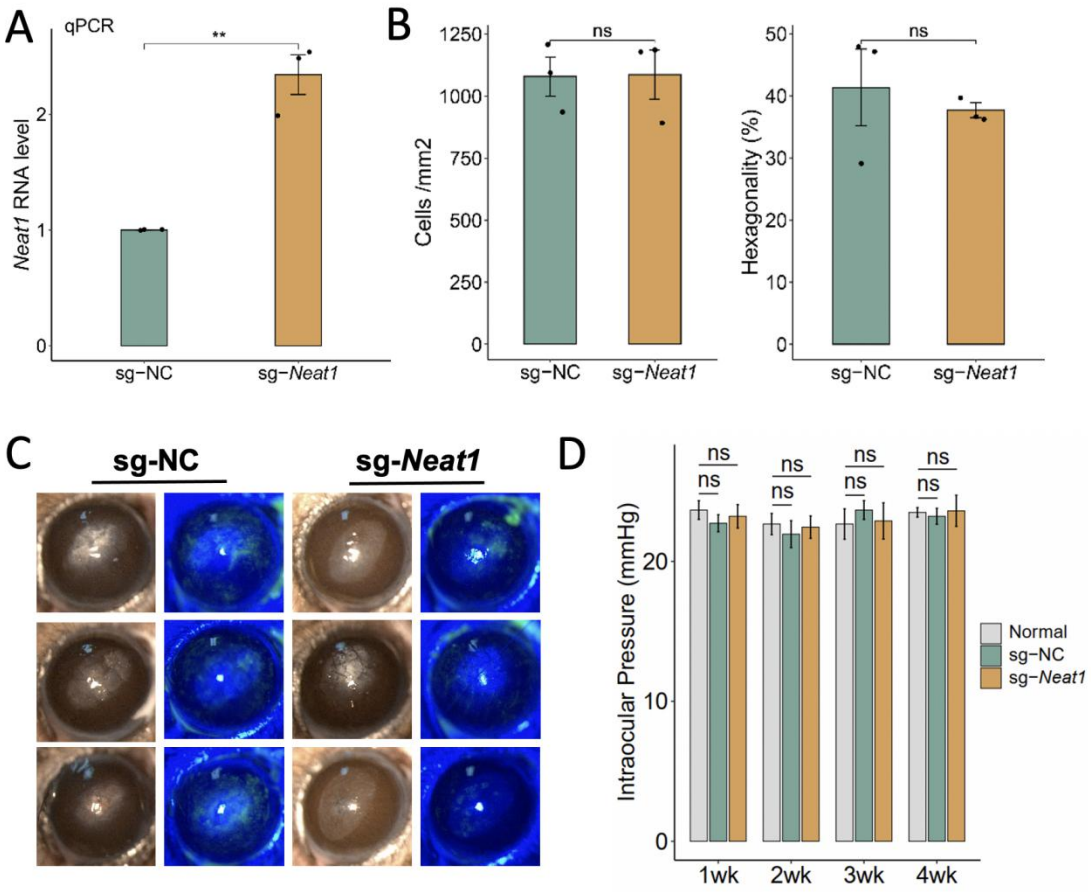

Figure S8. *Neat1*-targeting CRISPR-dCas9 activation system up-regulates expression of *Neat1* in mouse CE. (A) qRT-PCR verified the upregulation of *Neat1* (n=3). **, $p<0.01$ (two-tailed t test). (B) Cell density and hexagonality for CE treated with sg-NC and sg-*Neat1* rAAV (n=3). ns, not significant . (C) Representative slit lamp images showing corneal clarity and fluorescein staining of the corneal epithelial surface 3 months post 500 J/cm^2 UVA. (D) Barplot showing rAAV activating *Neat1* expression has no effect on intraocular pressure (IOP) in treated and control eyes (n=6). ns, not significant (two-tailed t test).

Supplemental Tables

Table S1 (xls). Details for donor cornea samples.

Table S2 (xls). DEGs for different cell clusters of human corneal endothelium.

Table S3 (xls). Target sequences for AAVs and LVs.

Table S4 (xls). Primer sequences for RT-PCR.